



Lab Resource: Genetically-Modified Multiple Cell Lines

Generation and heterozygous repair of human iPSC lines from three individuals with cerebellar ataxia, neuropathy and vestibular areflexia syndrome (CANVAS) carrying biallelic AAGGG expansions in *RFC1*

Kayli C. Davies ^{a,b}, Kiymet Bozaoglu ^{a,b}, Paul J. Lockhart ^{a,b,*}^a Murdoch Children's Research Institute, Parkville, Australia^b Department of Paediatrics, University of Melbourne, Parkville, VIC, Australia

A B S T R A C T

Cerebellar ataxia, neuropathy, and vestibular areflexia syndrome (CANVAS) is a progressive neurodegenerative disorder predominantly caused by biallelic AAGGG expansions in the second intron of the *RFC1* gene. Here, we used a simultaneous reprogramming and CRISPR-Cas9 genome editing approach to generate three patient iPSC lines with homozygous AAGGG expansions along with three heterozygous gene corrected iPSC lines. The iPSC lines expressed pluripotency markers, had a normal karyotype, and were able to differentiate into all three embryonic germ layers. These mutant and corrected iPSC lines will be a valuable tool for studying the molecular mechanisms underlying CANVAS.

1. Resource table

	(continued)	
Unique stem cell lines identifier	Clonality	Clonal
	Evidence of the reprogramming transgene loss (including genomic copy if applicable)	PCR
	Cell culture system used	Essential 8 Medium on Matrigel-coated plates
Alternative name(s) of stem cell lines	Type of Genetic Modification	Heterozygous Gene Correction
	Associated disease	Cerebellar ataxia, neuropathy, and vestibular areflexia syndrome (OMIM: 614575)
	Gene/locus	<i>RFC1/AAGGG</i> _(exp)
	Method of modification/site-specific nuclease used	CRISPR/Cas9
	Site-specific nuclease (SSN) delivery method	Plasmid transfection
Institution	All genetic material introduced into the cells	Reprogramming and gene editing plasmids
	Analysis of the nuclease-targeted allele status	Sequencing of the targeted allele, Repeat primed-PCR for the untargeted allele
Contact information of the reported cell line distributor	Method of the off-target nuclease activity surveillance	N/A
Type of cell lines	Name of transgene	N/A
Origin	Eukaryotic selective agent resistance (including inducible/gene expressing cell-specific)	N/A
Additional origin info (applicable for human ESC or iPSC)	Inducible/constitutive system details	N/A
Cell Source	Date archived/stock date	May 2021
Method of reprogramming	Cell line repository/bank	

(continued on next column)

(continued on next page)

* Corresponding author at: Murdoch Children's Research Institute, 50 Flemington Road Parkville, Victoria 3052, Australia.

E-mail address: paul.lockhart@mcri.edu.au (P.J. Lockhart).

(continued)

Ethical/GMO work approvals	https://hpscreg.eu/cell-line/MCRIi025-A
Addgene/public access repository recombinant DNA sources' disclaimers (if applicable)	This study was approved through the Human Research Ethics Committee of the Royal Children's Hospital (HREC 28097), Victoria, Australia pEP4 E025 ET2K (Addgene plasmid #20927) pEP4 E025 EN2L (Addgene plasmid #20922) pEP4 E025 EM2K (Addgene plasmid #20923) pSimple-miR302/367 (Addgene plasmid #98748) pSMART-sgRNA(Sp) (Addgene plasmid #80427) pSP6-EBNA ^{2A+DBD} (Addgene plasmid #98749) pDNR-SpCas9-Gem (Addgene plasmid #80424)

2. Resource utility

Biallelic expansion of an AAGGG repeat in *RFC1* is one of the most common genetic causes of late-onset ataxia. We generated three patient-derived iPSC lines carrying biallelic *RFC1* expansions and corresponding heterozygous gene corrected isogenic lines that will provide an important model for understanding the disease mechanisms underlying *RFC1*-mediated ataxia (see Table 1).

3. Resource details

Cerebellar ataxia, neuropathy, and vestibular areflexia syndrome (CANVAS) is a late-onset, slowly progressive, neurodegenerative disorder characterised by the triad of cerebellar impairment, bilateral vestibular hypofunction and somatosensory abnormalities. Recently, biallelic expansions of an AAGGG repeat in intron 2 of the replication factor C subunit 1 (*RFC1*) gene were identified as the cause of CANVAS and a common cause of other late-onset ataxias (Cortese et al., 2019; Rafehi et al., 2019). The molecular mechanisms underlying biallelic *RFC1* expansions are currently unknown and there are no disease-modifying treatments available. Therefore, there is a need to develop cellular models to investigate disease pathogenesis and identify potential therapeutic targets.

Here we describe the generation of iPSC lines from three unrelated individuals (CANVAS1-2, CANVAS3-2, and CANVAS4-6) with homozygous AAGGG expansions in *RFC1* (Rafehi et al., 2019). Using a simultaneous reprogramming and CRISPR/Cas9 gene editing approach (Howden et al., 2018), we also generated matched heterozygous gene corrected isogenic lines where one of the AAGGG expansions was deleted (Fig. 1A). Episomal reprogramming vectors, *in vitro* transcribed mRNA encoding SpCas9, and two sgRNAs flanking the AAGGG expansion in *RFC1* were co-transfected into fibroblasts derived from three individuals with CANVAS. iPSC colonies were isolated, expanded, and screened using PCR primers flanking the Cas9-target sites to identify edited clones where the large AAGGG expansion and approximately 350 base pairs of intron 2 of *RFC1* have been deleted (Fig. 1A). Successfully edited clones were identified by the presence of an ~ 255 base pair band (Fig. 1B) while unedited clones did not generate a PCR product, as

expected due to the large expansion. Deletion of the AAGGG expansion was confirmed by sanger sequencing (Fig. 1C-D). Repeat-primed PCR (RP-PCR) specific for the AAGGG expansion generated a characteristic sawtooth pattern, demonstrating the presence of at least one expanded allele in all lines (Fig. 1E). Collectively, these analyses confirm the generation of heterozygous gene corrected and homozygous uncorrected iPSC clones.

Flow cytometry analysis of MCRIi025-A (C1-2), MCRIi025-B (C1-2 Het GC), MCRIi026-A (C3-2), MCRIi026-B (C3-2 Het GC), MCRIi027-A (C4-6), and MCRIi027-B (C4-6 Het GC) showed that >91 % of the cell populations expressed the pluripotency markers TRA-1-60, SSEA4, and OCT3/4 (Fig. 1F). In addition, all lines all displayed normal iPSC morphology including the formation of compact colonies, an increased nuclear-cytoplasmic ratio, and prominent nucleoli (Fig. 1G). Immunofluorescence staining for markers OCT4 and NANOG further confirmed pluripotency of the cells (Fig. 1H). The ability of the cell lines to differentiate into cells from all three embryonic germ layers *in vitro* was demonstrated via the formation of embryoid bodies. Expression of ectoderm marker MAP2, mesoderm marker SMA, and endoderm marker SOX17 was confirmed by immunofluorescence staining in all iPSC lines (Fig. 1I). SNP array analysis of all six lines confirmed there were no aneuploidies or large deletions or insertions present (Supplementary Fig. 2). SNPduo comparison confirmed >99.9 % identity between the iPSC lines and their parental fibroblast line (Supplementary Fig. 3–5). All iPSC lines were confirmed to be free from mycoplasma contamination (Supplementary Fig. 6).

4. Materials and methods

4.1. Cell culture

Fibroblasts were maintained in DMEM (ThermoFisher Scientific) supplemented with 15 % fetal bovine serum (FBS). All iPSCs were cultured on Matrigel-coated (Corning) plates in Essential 8 (E8) medium (ThermoFisher Scientific). Cells passaged (1:3–1:6) every 3–4 days with 0.5 mM EDTA and cultured at 37 °C and 5 % CO₂.

4.2. Reprogramming and Cas9-mediated gene editing

Neon transfection system (ThermoFisher Scientific) was used for simultaneous reprogramming and gene correction, described in detail by Howden et al. (Howden et al., 2018). Briefly, primary fibroblasts were harvested with TrypLE (ThermoFisher Scientific) and 1 × 10⁶ cells were resuspended in Buffer R. 100 µL of cell suspension was added to a tube containing plasmids required for reprogramming and gene editing (Table 2), *in vitro* transcribed mRNA encoding SpCas9, and mRNA encoding EBNA1 to enhance nuclear uptake of the plasmids. Electroporation was performed at 1400 V, 20 ms, two pulses. Electroporated cells were plated on Matrigel-coated 6-well plates in fibroblast medium for 3 days post-transfection then switched to E8 medium (ThermoFisher Scientific) containing 100 µM sodium butyrate and changed every other day. After the appearance of iPSC colonies (day 14), media was switched to E8, individual colonies isolated and expanded. Cells were characterised at passage 5–10 as follows.

4.3. PCR screening and mutation analysis

For screening of corrected clones, gDNA was extracted using a DNAeasy Blood and Tissue Kit (Qiagen) following manufacturer's instructions. PCR was performed with a standard 65TD60 protocol using GoTaq Green Mastermix (Promega) and primers flanking the Cas9-target sites (Table 2). PCR products were analysed by gel electrophoresis followed by Sanger sequencing. AAGGG expansions in *RFC1* were confirmed by RP-PCR, performed as previously described (Cortese et al., 2019).

Table 1
Characterization and validation.

Classification	Test	Result	Data
Morphology	Photography	Normal	Fig. 1G (scale bar 100 μm)
Pluripotency status evidence for the described cell line	Qualitative analysis (Immunofluorescence) Quantitative analysis (Flow cytometry)	All lines OCT4 and NANOG positive TRA-1-60 & OCT3/4: >91% SSEA4 & OCT3/4: >92%	Fig. 1H (scale bar 20 μm) Fig. 1F
Karyotype	SNP array (0.5 Mb resolution)	C1-2: 46XX C1-2 Het GC: 46XX C3-2: 46XX C3-2 Het GC: 46XX C4-6: 46XY C4-6 Het GC: 46XY No aneuploidies were detected.	Supplementary Fig. 2
Genotyping for the desired genomic alteration/allelic status of the gene of interest	PCR across the edited site or targeted allele-specific PCR	Heterozygous deletion of AAGGG expansion determined by PCR and confirmed by Sanger sequencing in lines C1-2 Het GC, C3-2 Het GC, and C4-6 Het GC. RP-PCR confirmed the presence of an unedited allele.	Fig. 1B-E
Verification of the absence of random plasmid integration events	Transgene-specific PCR PCR	N/A PCR targeting the ampR gene present on all episomal reprogramming vectors. No integration.	N/A Supplementary Fig. 1
Parental and modified cell line genetic identity evidence	STR analysis, microsatellite PCR (mPCR) or specific (mutant) allele seq	SNPduo comparative analysis performed to compare mutant iPSC and gene edited iPSC clones to parental fibroblast line. Identical genotypes (>99.9%) for the entire genome, indicating cell lines are from the same individual	Supplementary Figs. 3-5 Supplementary Figs. 3-5
Mutagenesis / genetic modification outcome analysis	Sequencing (genomic DNA PCR or RT-PCR product) PCR-based analyses Southern Blot or WGS; western blotting (for knock-outs, KOs)	Sanger sequencing tracks with comparison to reference genome sequence. N/A N/A	Fig. 1C-D N/A N/A
<i>Off-target nuclease analysis-</i>	PCR across top 5/10 predicted top likely off-target sites, whole genome/exome sequencing	N/A	N/A
Specific pathogen-free status	Mycoplasma	Mycoplasma testing by PCR. Negative.	Supplementary Fig. 6
Multilineage differentiation potential	Embryoid body formation (immunofluorescence)	Expression of ectoderm (MAP2), mesoderm (SMA), and endoderm (SOX17) markers.	Fig. 1I (scale bar 20 μm)
<i>Donor screening (OPTIONAL)</i>	HIV 1 + 2 Hepatitis B, Hepatitis C	N/A	N/A
<i>Genotype – additional histocompatibility info (OPTIONAL)</i>	Blood group genotyping HLA tissue typing	N/A N/A	N/A N/A

4.4. Immunofluorescence

Following fixation in 4 % paraformaldehyde for 10 min at room temperature, cells were permeabilized for 10 min in 0.2 % Triton X-100, then blocked in 2 % bovine serum albumin for 60 min. Cells were then incubated overnight at 4 °C with primary antibodies, followed by 60 min incubation with secondary antibodies at room temperature (Table 2). Coverslips were mounted on slides with DAPI (Vectashield®) to counterstain the nuclei and imaged on an LSM 780 confocal microscope (Zeiss).

4.5. Flow cytometry

Cells were harvested using TrypLE and incubated with conjugated antibodies to TRA-1-60 and SSEA4 (Table 2) diluted in PBS containing 2 % FBS at 4 °C for 15 mins. Cells were then fixed with Foxp3 fixation/permeabilization buffer (ThermoFisher Scientific) and stained with a conjugated OCT3/4 antibody (Table 2). Samples were analyzed with an LSR II flow cytometer and FlowJo software.

4.6. Embryoid body (EB) formation

iPSCs were plated in ultra-low attachment 96-well plates (Corning) and cultured for 24 h in E8 media with 0.5 % polyvinyl alcohol (Sigma). Thereafter, cells were cultured in E8 media. After 2 weeks, cells were plated onto Matrigel-coated chamber slides and cultured in E8 media for

2 weeks prior to analysis by immunofluorescence.

4.7. Molecular karyotyping and genetic evidence of identity

Karyotyping was performed by the Victorian Clinical Genetics Service (Murdoch Children's Research Institute, Melbourne, Australia) using an Illumina Infinium GSA-24 v2.0 SNP array. STR analysis was not performed to confirm genetic identity. Instead, SNPduo analysis was performed (<https://pevsnerlab.kennedykrieger.org/SNPduo/>). This highly sensitive methodology compared >600,000 SNPs between parental fibroblast and iPSC lines, including SNPs within *RFC1*, to validate genetic identity.

4.8. Mycoplasma testing

Absence of mycoplasma contamination in the iPSCs was confirmed by PCR, performed by Cerberus Sciences (Adelaide, Australia).

Declaration of Competing Interest

The authors declare the following financial interests/personal relationships which may be considered as potential competing interests: Paul J Lockhart reports a relationship with Orion Biotechnology LLC that includes: consulting or advisory.

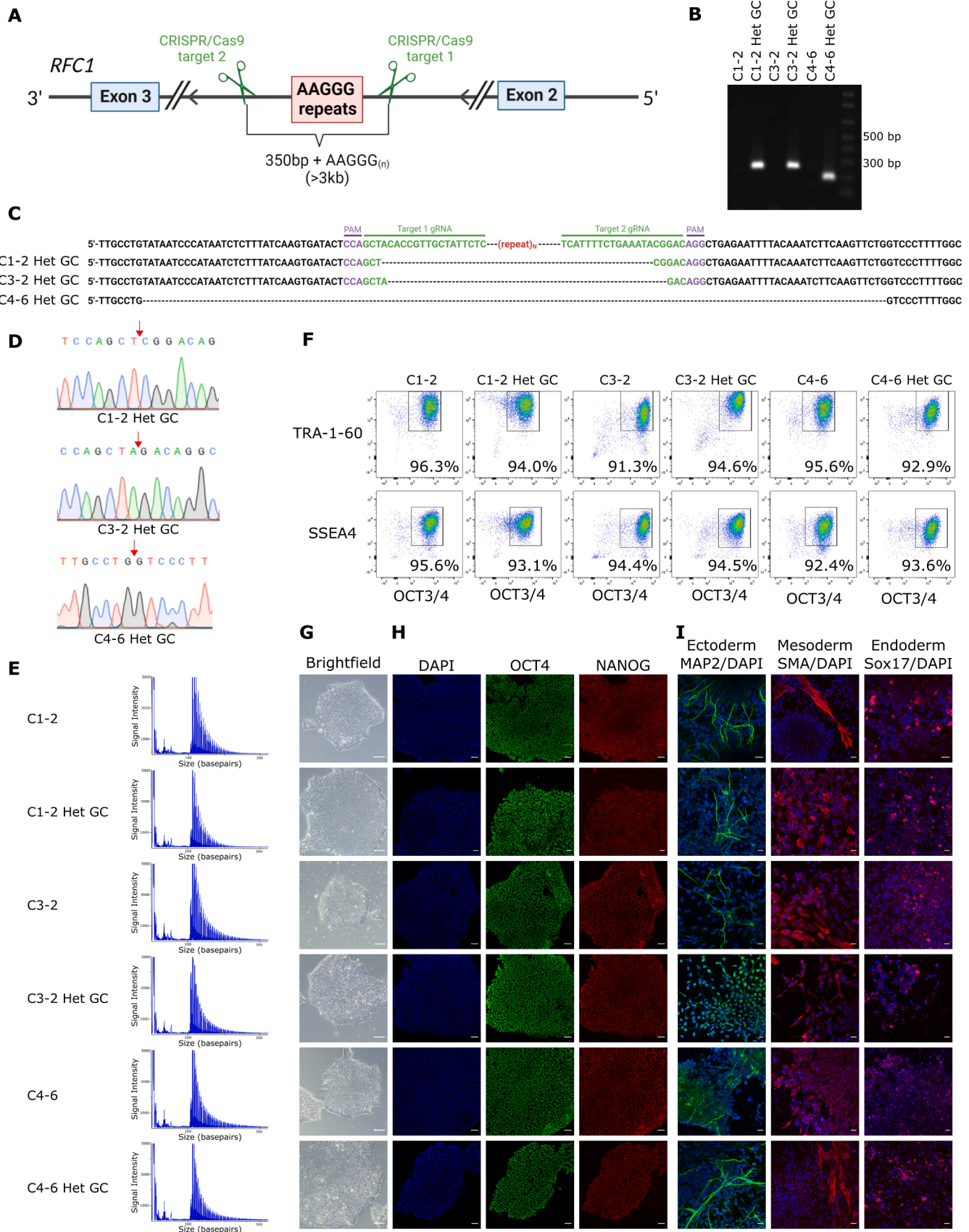


Fig. 1.

Table 2
Reagents details.

Antibodies and stains used for immunocytochemistry/flow-cytometry			
	Antibody	Dilution	Company Cat # and RRID
Pluripotency Markers	Rabbit anti-Oct-4A monoclonal antibody (C30A3)	1:400	Cell Signaling Technology Cat#2840 RRID: AB_2167691
Pluripotency Markers	Mouse anti-Nanog monoclonal antibody	1:400	BioLegend Cat# 674202, RRID:AB_2564574
Pluripotency Markers	BV421 Mouse anti-Human TRA-1–60 antibody	1:20	BD Biosciences Cat# 562711, RRID: AB_2737738
Pluripotency Markers	Alexa Fluor 647Anti-Human SSEA-4 antibody	1:100	BioLegend Cat# 330408, RRID:AB_1089200
Pluripotency Markers	PE Mouse anti-OCT3/4	1:5	BD Biosciences Cat# 560186, RRID: AB_1645331
Differentiation Markers	Chicken anti-MAP2 Polyclonal Antibody	1:5000	Abcam Cat# ab5392, RRID:AB_2138153
Differentiation Markers	Goat anti-SOX17 Polyclonal Antibody	1:50	Santa Cruz Biotechnology Cat# sc-17355, RRID: AB_2239898
Differentiation Markers	Monoclonal Mouse Anti Human Smooth Muscle Actin Antibody	1:25	Agilent Cat# M0851, RRID:AB_2223500
Secondary Antibodies	Goat anti-Rabbit IgG (H + L) Cross-Adsorbed Antibody, Alexa Fluor 488	1:1000	Thermo Fisher Cat# A-11008, RRID:AB_143165
Secondary Antibodies	Goat anti-Mouse IgG (H + L) Highly Cross-Adsorbed Antibody, Alexa Fluor 594	1:1000	Thermo Fisher Cat# A-11032, RRID: AB_2534091
Secondary Antibodies	Goat anti-Chicken IgY (H + L) Antibody, Alexa Fluor 488	1:1000	Thermo Fisher Cat# A-11039, RRID:AB_142924
Secondary Antibodies	Donkey anti-Goat IgG (H + L) Cross-Adsorbed Antibody, Alexa Fluor 647	1:1000	Thermo Fisher Cat# A-21447, RRID:AB_141844
Site-specific nuclease			
Nuclease information	CRISPR/Cas9		pDNR-SpCas9-Gem (Addgene #80424)
Delivery method	Electroporation		Thermo Fisher Neon Transfection System
Selection/enrichment strategy	N/A		
Primers and Oligonucleotides used in this study			
	Target		Forward/Reverse primer (5'-3')
sgRNA	RFC1 intron 2 Cas9 cut sites		GCTACACCGTTGCTATTCTC / TCATTTCTGAAATACGGAC
Genotyping – Deletion detection and sequencing	Edited allele-specific PCR		CTGTGTTGTCCTGCACTGG / GCCTGAGTCCTCCTGACTGCG
Targeted mutation analysis – RP-PCR forward and anchor primers	AAGGG repeat expansions in RFC1		6FAM-5'-TCAAGTGATACTCCAGCTACACCGT / CAGGAACAGCTATGACCAACAGAGCAAGACTCTGT
Targeted mutation analysis – RP-PCR reverse primers	AAGGG repeat expansions in RFC1		CAGGAAACAGCTATGACCAACAGAGCAAGACTCTGT TTCAAAAAGGGAAGGGAAGGGAAGGGAA / CAGGAAACAGCTATGACCAACAGAGCAAGACTCTGT TTCAAAAAGGGAAGGGAAGGGAAGGGAA / CAGGAAACAGCTATGACCAACAGAGCAAGACTCTGT TTCAAAAAGGGAAGGGAAGGGAAAGGGAA
Reprogramming and gene editing plasmids			
	Plasmid		Company Cat #
Reprogramming	pEP4 E02S ET2K		Addgene plasmid #20927
Reprogramming	pEP4 E02S EN2L		Addgene plasmid #20922
Reprogramming	pEP4 E02S EM2K		Addgene plasmid #20923
Reprogramming	pSimple-miR302/367		Addgene plasmid #98748
Genome editing	pSMART-sgRNA(Sp)		Addgene plasmid #80427
Reprogramming	pSP6-EBNA ^{2A+DBD}		Addgene plasmid #98749
Genome editing	pDNR-SpCas9-Gem		Addgene plasmid #80424

Data availability

Data will be made available on request.

Acknowledgements

We would like to thank the participants and their families for participating in our research. This work was supported by the Australian Government National Health and Medical Research Council grant (GNT2001513) to P.J.L. Additional funding was provided by the Independent Research Institute Infrastructure Support Scheme and the Victorian State Government Operational Infrastructure Program. K.C.D is supported by an Australian Research Training Program Scholarship. K.B was supported by an E.H. Flack Fellowship, and P.J.L was supported by the Vincent Chiodo Foundation. The MCRI iPSC Core Facility is

supported by the Stafford Fox Medical Research Foundation.

Appendix A. Supplementary data

Supplementary data to this article can be found online at <https://doi.org/10.1016/j.scr.2023.103047>.

References

- Cortese, A., Simone, R., Sullivan, R., Vandrovčová, J., Tariq, H., Yau, W.Y., Humphrey, J., Jaunmuktane, Z., Sivakumar, P., Polke, J., Ilyas, M., Tribollet, E., Tomaselli, P.J., Devigili, G., Callegari, I., Versino, M., Salpietro, V., Efthymiou, S., Kaski, D., Wood, N.W., Andrade, N.S., Buglo, E., Rebelo, A., Rossor, A.M., Bronstein, A., Fratta, P., Marques, W.J., Züchner, S., Reilly, M.M., Houlden, H.,

2019. Biallelic expansion of an intronic repeat in RFC1 is a common cause of late-onset ataxia. *Nat. Genet.* 51, 649–658.
- Howden, S.E., Thomson, J.A., Little, M.H., 2018. Simultaneous reprogramming and gene editing of human fibroblasts. *Nat. Protoc.* 13, 875–898.
- Rafehi, H., Szmulewicz, D.J., Bennett, M.F., Sobreira, N.L.M., Pope, K., Smith, K.R., Gillies, G., Diakumis, P., Dolzhenko, E., Eberle, M.A., Barcina, M.G., Breen, D.P., Chancellor, A.M., Cremer, P.D., Delatycki, M.B., Fogel, B.L., Hackett, A., Halmagyi, G.M., Kapetanovic, S., Lang, A., Mossman, S., Mu, W., Patrikios, P., Perlman, S.L., Rosemberg, I., Storey, E., Watson, S.R.D., Wilson, M.A., Zee, D.S., Valle, D., Amor, D.J., Bahlo, M., Lockhart, P.J., 2019. Bioinformatics-based identification of expanded repeats: a non-reference intronic pentamer expansion in RFC1 causes CANVAS. *Am. J. Hum. Genet.* 105, 151–165.